

## MTSS1 is epigenetically regulated in glioma cells and inhibits glioma cell motility



Daniel Luxen<sup>\*,1</sup>, Gerrit H. Gielen<sup>\*,1</sup>, Anke Waha<sup>\*</sup>, Lukas Isselstein<sup>\*</sup>, Tim Müller<sup>\*</sup>, Philipp Koch<sup>‡</sup>, Jennifer Hammes<sup>\*</sup>, Albert Becker<sup>\*</sup>, Matthias Simon<sup>†</sup>, Peter Wurst<sup>§</sup>, Elmar Endl<sup>§</sup>, Torsten Pietsch<sup>\*</sup>, Marco Gessi<sup>\*,\*</sup> and Andreas Waha<sup>\*</sup>

<sup>\*</sup>Department of Neuropathology, University of Bonn, Germany; <sup>†</sup>Institute of Neurosurgery, University of Bonn, Germany; <sup>‡</sup>Institute of Reconstructive Neurobiology, *LIFE & BRAIN*, University of Bonn, Germany; <sup>§</sup>Department of Molecular Medicine and Experimental Immunology, (Core Facility Flow Cytometry) University of Bonn, Germany

### Abstract

Epigenetic silencing by DNA methylation in brain tumors has been reported for many genes, however, their function on pathogenesis needs to be evaluated. We investigated the *MTSS1* gene, identified as hypermethylated by differential methylation hybridization (DMH). Fifty-nine glioma tissue samples and seven glioma cell lines were examined for hypermethylation of the *MTSS1* promotor, *MTSS1* expression levels and gene dosage. GBM cell lines were treated with demethylating agents and interrogated for functional consequences of *MTSS1* expression after transient transfection. Hypermethylation was significantly associated with *IDH1/2* mutation. Comparative SNP analysis indicates higher incidence of loss of heterozygosity of *MTSS1* in anaplastic astrocytomas and secondary glioblastomas as well as hypermethylation of the remaining allele. Reversal of promoter hypermethylation results in an increased *MTSS1* expression. Cell motility was significantly inhibited by *MTSS1* overexpression without influencing cell growth or apoptosis. Immunofluorescence analysis of *MTSS1* in human astrocytes indicates co-localization with actin filaments. *MTSS1* is down-regulated by DNA methylation in glioblastoma cell lines and is part of the G-CIMP phenotype in primary glioma tissues. Our data on normal astrocytes suggest a function of *MTSS1* at focal contact structures with an impact on migratory capacity but no influence on apoptosis or cellular proliferation.

*Translational Oncology* (2017) 10, 70–79

### Introduction

Glioblastoma (GBM) is the most common primary brain tumor in adults, accounting for approximately 15% of all intracranial neoplasms and 60% of all astrocytic tumors. Due to very poor response to radiation and chemotherapy, the course of disease is dismal and average survival time is less than 2 years [1].

While the majority of glioblastomas arise *de novo* (primary glioblastomas), about 5% of GBM tumors develop through malignant progression of lower grade precursor lesions (secondary glioblastomas). Primary and secondary glioblastomas differ in genetic and epigenetic alterations. Primary glioblastomas frequently show *EGFR* amplification, *PTEN* mutations or *CDKN2A* deletions. Secondary glioblastomas present frequent mutations of the *TP53* and *IDH1* genes. Conversely, in adult disease both tumors frequently show 10q loss [2–4].

Epigenetic silencing of cancer-associated genes has been extensively studied in gliomas and data from recent comprehensive analyses of DNA methylation add to a constantly growing list of putative candidate genes in these tumors. Hypermethylation leads to the

Address all correspondence to Andreas Waha, PhD, Department of Neuropathology, University of Bonn Medical Center, Sigmund-Freud-Str. 25, D-53105 Bonn, Germany.

E-mail: [awaha@uni-bonn.de](mailto:awaha@uni-bonn.de)

<sup>†</sup>These authors contributed equally.

Received 13 May 2016; Revised 18 November 2016; Accepted 22 November 2016

© 2016 The Authors. Published by Elsevier Inc. on behalf of Neoplasia Press, Inc. This is an open access article under the CC BY-NC-ND license (<http://creativecommons.org/licenses/by-nc-nd/4.0/>).

1936-5233/17

<http://dx.doi.org/10.1016/j.tranon.2016.11.006>

“glioma associated CpG-island methylator phenotype” (G-CIMP) reported by Noushmehr et al. [5]. This phenotype is associated with *IDH1 R132* mutation that results in low amounts of  $\alpha$ -Ketoglutarate ( $\alpha$ -KG) and high levels of 2-hydroxyglutarate (2-HG). This oncometabolite inhibits TET (ten-eleven translocation) enzymes involved in demethylation of CpG dinucleotides ultimately leading to an accumulation of hypermethylated CpG sites in a large set of DNA sequences.

Using differential methylation hybridization (DMH) we previously performed a genome-wide methylation analysis to find new potential candidate genes in gliomas showing altered methylation profiles compared to normal human brain tissues [6]. One of these identified genes encodes the *metastasis-suppressor-1* (*MTSS1/MIM = missing in metastasis*) on chromosome 8q24.13.

MTSS1 is an actin-binding protein involved in cytoskeleton function. The protein contains a WASP-homology 2 (WH2) actin-binding motif and an IMD (IRSp53 MIM domain) which regulate cytoskeletal dynamics by restriction of actin polymerization [7–9].

MTSS1 is expressed in various tissues including spleen, thymus, prostate, uterus, colon or peripheral blood but absent or low expressed in different cancer types including bladder [10], gastric [11], colorectal [12] and breast cancer [13] where its reduced expression correlates with poor patient survival. In basal cell carcinomas *MTSS1* has also been identified as a Sonic Hedgehog (SHH) responsive gene, potentiating *Gli* dependent transcription [14]. Moreover, MTSS1 may regulate EGFR signaling [15].

DNA methylation of *MTSS1* and transcriptional silencing has been described by Utikal et al. in bladder cancer cell lines detecting a promoter activity region 276 bp upstream of the *MTSS1* gene within a CpG island [16]. In addition, Fan et al. described a DNA methylation independent silencing mechanism by DNA methyltransferase 3B (DNMT3B) in hepatocellular carcinomas [17]. Most recently Schemionek et al. described MTSS1 as an epigenetic regulated tumor suppressor in chronic myeloid leukemia (CML) [18].

So far, little information is available about the potential contribution of *MTSS1* to the biology of gliomas and the role of its epigenetic silencing is largely unknown. Given its function in regulating cell motility and migration it could be hypothesized that *MTSS1* could play a critical role driving tumor cell invasion [19].

In this study, we investigated the methylation and expression status of *MTSS1* and its potential prognostic significance in high-grade gliomas. Furthermore, we explored the potential role of *MTSS1* to regulate cell motility and invasion in glioma cell lines.

## Material and Methods

### Tumor Samples, Cell Lines and Reference Material

Formalin-fixed and paraffin embedded tumor specimens from 59 patients including 38 primary glioblastomas WHO grade IV, 10 secondary glioblastomas WHO grade IV and 11 anaplastic astrocytomas WHO grade III were included in the study. All tumors were diagnosed according to the 2007 World Health Organization (WHO) classification of tumors of the central nervous system [20].

As reference tissue for methylation analyses, four normal white matter brain tissues were used. All tissue samples were used in an anonymous manner as approved by the local ethics committee at the University of Bonn Medical Center. Human brain RNA samples from temporal, occipital, frontal and parietal lobe were supplied by BioChain Institute Inc. Hayward, CA, USA and two additional

human brain RNA samples from Stratagene, La Jolla, CA, USA; BD Biosciences St. Jose, CA, USA.

### Blood Samples

Lymphocytes DNA of all 59 patients including mentioned 38 primary glioblastomas, 10 secondary glioblastomas and 11 anaplastic astrocytomas were included in the study. Blood samples also were used in an anonymous manner as approved by the local ethics committee at the University of Bonn Medical Center.

### DNA/RNA Extraction

Tumor tissues were selected for DNA extraction after careful examination of corresponding hematoxylin-eosin-stained sections. All samples contained at least 80% of vital tumor. Extraction of DNA and RNA was carried out as described [21]. For all tumor specimens matched formalin-fixed and paraffin-embedded tumor tissues were available for immunostaining.

### MTSS1 Methylation Analysis

Genomic DNA 0.5  $\mu$ g was treated with sodium bisulfite using the EpiTect Bisulfite kit (Qiagen, Hilden, Germany) according to manufacturer's recommendations. A pyrosequencing assay was developed that targets 11 CpG positions in a CpG island 5' of the *MTSS1* gene, which was detected in the DMH assay. Primer sequences were *MTSS1*-bf-4 5'-TAAAGAGGAGTTTGTGTTGTTGTT-3' and *MTSS1*-br-4 5'-ACAATCCTAACATCAAAAAATAAA-3' yielding a PCR product of 323 bp. The reverse primer was biotinylated at the 5' position. PCR conditions were 10 min. at 95°C following 40 cycles of 94°C, 54°C and 72°C each 45 sec and finally 72°C for 10 min.

Single-stranded DNA templates of this PCR product were immobilized on streptavidin-coated sepharose high-performance beads (GE Healthcare, Uppsala, Sweden) using the PSQ Vacuum Prep Tool and Vacuum Prep Worktable (Biotage, Uppsala, Sweden), according to manufacturer's instructions, then incubated at 80°C for 2 minutes and annealed to 0.4 mM sequencing primer *MTSS1*-pyro01 5'-TTTATTTTATAATGGTT-3'. Pyrosequencing was performed using PyroGold Reagents (Biotage, Uppsala, Sweden) on the Pyromark Q24 instrument (Biotage, Uppsala, Sweden), according to manufacturer's instructions. Pyrogram outputs were analyzed using the PyroMark CpG quantification software (Biotage, Uppsala, Sweden) to determine the percentage of methylated *versus* unmethylated alleles according to the percentage of respective relative peak height. The overall methylation level was determined by taking the mean of the arithmetic point of the pyrosequencing methylation data from all 11 CpG positions. White matter samples showed traces of methylation (-4%) and were, therefore, scored not methylated. Tumor samples were scored negative if they did not exceed the eight-fold SD of white matter control samples (13.79%).

### Cell Culture and Treatment with 5-aza-2'-deoxycytidine

Glioma cell lines A172, U373MG, T98G, U178, LN428, U87MG and LN229, were obtained from the LICR (San Diego, USA) and cultured as described [22]. Identities were confirmed by STR DNA profiling of 15 loci plus sex determining marker amelogenin (Genetica DNA Laboratories). To induce DNA demethylation, cell lines were treated with 0.5  $\mu$ M 5-aza-2'-deoxycytidine for 3 days, and DNA as well as total RNA was extracted for *MTSS1* methylation and expression analysis.

**Table 1.** Summary of *MTSS1* Methylation, *IDH1* Mutation, LOH and Survival Data of Investigated Gliomas

Number	Sample ID	Diagnosis	MTSS1 Methylation Status	IDH1/2 Mutation Status	L O H / MOH	OS (d)
1	T2494	pGBM	UM	wt	LOH	420
2	T2104	pGBM	UM	wt	MOH	510
3	T71	pGBM	UM	wt	n.i.	330
4	T2643	pGBM	UM	wt	n.i.	480
5	T1464	pGBM	UM	wt	n.i.	750
6	T3555	pGBM	UM	wt	n.i.	480
7	T2854	pGBM	UM	wt	LOH	420
8	T3070	pGBM	UM	wt	MOH	450
9	T2169	pGBM	UM	wt	n.i.	690
10	T2757	pGBM	UM	wt	n.i.	210
11	T2735	pGBM	UM	wt	n.i.	300
12	T2481	pGBM	UM	wt	n.i.	450
13	T2896	pGBM	UM	wt	MOH	120
14	T1968	pGBM	UM	wt	n.i.	90
15	T625	pGBM	UM	wt	n.i.	120
16	T1477	pGBM	UM	wt	n.i.	1020
17	T3513	pGBM	UM	wt	MOH	600
18	T3007	pGBM	UM	wt	n.i.	1050
19	T1010	pGBM	UM	wt	n.i.	90
20	T1619	pGBM	UM	wt	MOH	150
21	T862	pGBM	UM	wt	n.i.	90
22	T327	pGBM	UM	wt	n.i.	240
23	T3066	pGBM	UM	wt	MOH	990
24	T72	pGBM	UM	wt	MOH	240
25	T579	pGBM	M	wt	MOH	1110
26	T2884	pGBM	M	wt	MOH	660
27	T2486	pGBM	M	wt	n.i.	180
28	T2304	pGBM	M	wt	MOH	1020
29	T27	pGBM	M	wt	MOH	210
30	T3032	pGBM	M	mut	MOH	480
31	T3031	pGBM	M	wt	n.i.	300
32	T2887	pGBM	M	mut	MOH	780
33	T2881	pGBM	M	wt	MOH	960
34	T132	pGBM	M	wt	MOH	240
35	T820	pGBM	M	mut	MOH	1146
36	T1311	pGBM	M	wt	n.i.	150
37	T172	pGBM	M	wt	MOH	270
38	T2655	pGBM	M	mut	MOH	6840
39	T3548	AIII	UM	wt	MOH	n.a.
40	T3545	AIII	UM	wt	MOH	n.a.
41	T3546	AIII	M	mut	MOH	n.a.
42	T2899	AIII	M	mut	n.i.	n.a.
43	T2526	AIII	M	n.d.	MOH	n.a.
44	T2771	AIII	M	mut	MOH	n.a.
45	T2744	AIII	M	mut	MOH	n.a.
46	T2377	AIII	M	mut	n.i.	1410
47	T3423	AIII	M	mut	MOH	n.a.
48	T2897	AIII	M	mut	LOH	n.a.
49	T2725	AIII	M	mut	LOH	n.a.
50	T1944	sGBM	UM	mut	n.i.	3930
51	T2007	sGBM	UM	wt	n.i.	750
52	T677	sGBM	M	wt	n.i.	660
53	T1430	sGBM	M	wt	MOH	1440
54	T3475	sGBM	M	mut	n.i.	n.a.
55	T3527	sGBM	M	mut	MOH	990
56	T1214	sGBM	M	mut	LOH	2760
57	T1329	sGBM	M	mut	MOH	3540
58	T2727	sGBM	M	mut	LOH	1110
59	T2250	sGBM	M	mut	MOH	3780

### Comparative SNP Analysis

Two single nucleotide polymorphisms (SNP1: rs3763542 chr.8: 125,573,770; SNP2: rs3763543; chr. 8: 125,573,873) between the *MTSS1* gene exon 10 and 11 were chosen to detect potential losses of heterozygosity by comparing genomic DNA of matched tumor and lymphocyte DNA. We developed a pyrosequencing assay with primer sequences: *MTSS1*-SNP1+ 2-fw 5'-AGTTGCTAGCCACG CATGTC-3' and *MTSS1*-SNP1+ 2-rev 5'-TGCCTGACG

CCCCTTTCTG-3' yielding a PCR product of 179 bp. PCR conditions were 95°C for 20 sec and 50 cycles at 60°C for 30 sec and 95°C for 15 sec. PCR finishing was made by 95°C for 15 sec, 60°C for 60 sec, 95°C for 15 sec and 60°C for 15 sec. Following PCR single strand templates were purified as described above. These single strand templates were sequenced with the sequencing primers *MTSS1*-SNP1-py: 5'-CCCTCTTCTGCTTCC-3' and *MTSS1*-SNP2-py: 5'-GGCTGCAGCACGTGG-3'. 35 informative tumor tissue samples were used for this assay, in detail 25 of SNP: rs3763542 and 30 of SNP: rs3763543, 20 samples were informative in both SNP's, including 9 AIII, 6 sGBM and 20 pGBM (Supplementary Fig. 1, Table 1).

### *MTSS1* Transfection

*MTSS1*-pEGFP-C1 plasmid was provided by Dr. Laura Machesky, Glasgow, UK. LN229 cells were transfected by lipofection (HP transfection reagents, Roche) and selected by adding 500 µg/ml G418 to the growth medium after 24 hours. After 2 weeks G418 resistant clones were isolated and screened for *MTSS1* expression. Stable expression was confirmed by real-time-RT-PCR. Positive cells were expanded and used for Trans-Well-Invasion- and wounding-assay.

### Wounding/Motility Assay (Scratch Assay)

$1.5 \times 10^5$  LN229 cells stably expressing *MTSS1*-pEGFP-C1 or empty vector were seeded in 6 well plates and cultivated for 48 hours to reach confluency. The layer of cells was scraped with a pipette tip to create a wound. Cell debris was removed by washing with phosphate-buffered saline. The medium supplemented with 5% fetal calf serum was added and closure of the scratch was recorded after 0, 12, and 24 h using light microscopy and a digital camera. Three images were taken per well. The experiments were performed in duplicates.

### Invasion Assay (Trans-Well-Assay)

Invasion assays were performed with stably transfected LN229 cells transfected with the *MTSS1*-pEGFP-C1 or pEGFP-C1.  $1 \times 10^4$  cells were seeded on cell culture inserts (6.5 mm) with 8 µm pores (Transwell Permeable Supports, Corning life sciences, Amsterdam) according to the manufacturer's instructions and the cells were incubated for 10 hours. After 2 and 10 hours cells that had invaded through the basement membrane were fixed in 4% formaldehyde and washed twice in PBS. After every washing step the upper side of the membrane was cleaned with a cotton swap to remove upper cells. Migrated cells on the bottom side were stained with DAPI (1:5000) and covered on slides with vectorstain fluorescence mounting medium (Vector Laboratories Inc., Burlingame, USA). Migrated cells were counted using Axio-Imager 2.1 and associated software from Carl Zeiss (Axio Cam, Imager Z1 and Zeiss ApoTome, Axio Vision 4.8.2 Software). Four separate visual fields (0.4 mm<sup>2</sup>) were counted to determine the mean number of invaded cancer cells. The experiment was performed in triplicates.

### Measurement of Cellular Proliferation and Viability by Flow Cytometry

$5 \times 10^5$  LN229 cells were seeded in 25 ml culture vessels and transiently transfected with *MTSS1*-pEGFP-C1 plasmid or pEGFP-C1 control vector and cultivated for 48 hours. Flow cytometric immunophenotyping was done as described elsewhere [22,23]. Analysis was performed using a FACS Canto II flow cytometer (BD Biosciences, Heidelberg, Germany). Data were

analyzed using Flowjo (Tree Star, OR, USA) analysis software. At least 20,000 events were recorded per experiment. Only GFP expressing single cells were included in the analysis. Each experiment was carried out in duplicates.

### *IDH1 Mutation Analysis by Pyrosequencing*

Somatic sequence alterations of the codon R132 (*IDH1*) and R172 (*IDH2*) were investigated by pyrosequencing as described recently [24].

### *Differentiation of Human Astrocytes from IPS Cells and Immunofluorescence of MTSS1 in Astrocytes and U87MG Glioma Cells*

Astrocytes were derived from induced pluripotent stem cells generated from a 33-year old male donor as described elsewhere [25,26]. U87MG cells were transiently transfected with MTSS1-pKR5 plasmid by lipofection. Human astrocytes as well as MTSS1-pKR5-U87MG cells were fixed in PFA 4% for 20 min. The cells were permeabilized with TritonX100 (0.2%) in PBS for 15 min. The primary antibody (anti-MTSS1 1:250, Santa Cruz) was incubated at 4°C overnight. Phalloidin (1:40) was incubated at 21°C for 45 min. DAPI was used for nuclear staining. Pictures were taken with an Axioimager (Zeiss) with Apotome; sections of 6–12 µm with a 25× objective and 60× objective (Olympus Fluo View).

### *MTSS1 mRNA Expression Analysis by Real-Time Reverse Transcription-PCR*

*MTSS1* expression was investigated by real time reverse transcription-PCR using the ABI PRISM 5700 sequence detection system (Applied Biosystems). cDNA synthesis was performed with 1 µg of total RNA using random hexamers and SuperScript II Reverse Transcriptase (Invitrogen, Darmstadt, Germany) according to the instructions of the manufacturer. Transcript levels of *MTSS1* were normalized to the transcript levels of *ARF1* (ADP-ribosylation factor 1) and *PBDG* (porphobilinogen deaminase). Primer sequences were: MTSS1-rt.-f2, 5'-GGAGGCTGTGATTGAGAAGG-3' and MTSS1-rt.-r, 5'-AGCTGGGACTGCAGCTTTCC-3' located in exons 1 and 2 respectively yielding a PCR product of 129 bp. ARF1-f 5'-GACCACGATCCTCTACAAGC-3' and ARF1-r3 5'-TCCCACACAGTGAAGCTGATG-3' yielding a 190-bp fragment; PBDG-rt.-f1, 5'-TTCGCTGCATCGCTGAAAGG-3' and PBDG-rt.-r2 5'-CTCGTGGAAATGTTACGAGCA-3' producing a 688 bp cDNA specific PCR product.

Human brain RNA samples from temporal, occipital, frontal and parietal lobe as well as two additional human brain RNA samples were used as normal tissue controls and obtained from BioChain Institute Inc. Hayward, CA, USA and Stratagene, La Jolla, CA, USA; BD Biosciences St. Jose, CA, USA. White matter tissue samples showed an average expression ratio of MTSS1-RNA of 6.08 (normalized to the housekeeping gene ARF). Tissue samples therefore were scored positive within the mean of the arithmetic point of the white matter tissue plus/minus 2-fold SD (+/-2.39).

### *MTSS1 Immunohistochemistry in Formalin Fixed and Paraffin Embedded Tissue*

Paraffin embedded tissue specimens were cut at 4 µm serial sections on positively charged slides, routinely processed, air-dried overnight at 37°C, deparaffinized in xylene and rehydrated in a graded alcohol sequence. The slides were incubated in 3% hydrogen peroxide for 5 min at RT to block endogenous peroxidase activity and incubated in blocking solution (CSA II Kit, Dako, Glostrup,

Denmark) for 90 min at RT. Slides were incubated overnight with primary antibodies (Abnova 1:500). Slides were rinsed with TBST, bound antibody was detected using the CSA system antibodies technology (Dako CSA II, Biotin-Free Catalyzed Amplification System, Glostrup, Denmark) and visualized by diaminobenzidine tetrahydrochloride. The samples were counterstained with hematoxylin. Finally, the samples were dehydrated in a graded alcohol sequence and mounted in Richard-Allan Scientific Cytoseal XYL (Thermo Scientific, Waltham, MA, USA).

### *Statistical Analysis*

Statistical analyses were carried out with Prism Software Version 6 (GraphPad Software, Inc. and OrigeneLab Corporation, Northampton, MA, USA). Comparative  $C_t$  quantification (delta-delta ( $\Delta\Delta$ )  $C_t$ ) was applied. Experiments were performed in triplicates for *MTSS1* as well as the housekeeping gene *ARF1*. An unpaired t-test was applied to identify differences in *MTSS1* transcription between individual glioma cell lines from which *MTSS1* methylation status was available and from cells treated with the demethylating agent 5-aza-2'-deoxycytidine and respective controls. The results of the invasion assays comparing glioma cells with and without *MTSS1* protein expression were also statistically evaluated using unpaired *t* test. Correlation between molecular findings and individual glioma entities were calculated using Fisher's exact test. Clinical and molecular parameters were correlated with survival data using Kaplan-Meier survival and the Log-rank (Mantel-Cox) test (Fig. 6). OS time was defined as time between surgery for the primary tumor and death of the patient. Patients alive at the time of their last follow-up were censored.

## **Results**

### *Methylation of MTSS1 in Gliomas and IDH1 Mutational Status*

Using DMH analysis, we have previously identified a CpG rich fragment upstream of the start codon of the *MTSS1* gene (*MIM*, metastasis suppressor I) on chr.8 (125,563,028–125,740,730) showing *de novo* methylation in gliomas. To determine and verify the frequency of *de novo* methylation a specific pyrosequencing-based analysis was performed in a cohort of 59 glioma tissues comprising 38 primary glioblastomas (pGBM), 11 anaplastic astrocytomas (AAIII) and 10 secondary glioblastomas (sGBM). Seven glioblastoma cell lines were also analyzed. Representative hypermethylated and unmethylated tissue samples are shown in Fig. 1A.

*De novo* methylation was found in 14/38 (36.8%) pGBM, 9/11 (81.8%) AAIII and 8/10 (80%) sGBM, as showed in Fig. 1B. This data indicates a significant higher methylation frequency of *MTSS1* in sGBM compared to pGBM (Fisher's exact test 0.0293, Table 1). Secondary glioblastomas (WHO grade IV) and anaplastic astrocytomas (WHO grade III) show very similar methylation levels (*t*-test: 0.9164). As showed in Fig. 2A, *MTSS1* hypermethylation in 6 of 7 lines was observed: only U87MG cells show no *MTSS1* methylation. *IDH1* mutation was found in 4/38 pGBM (10.5%), 8/10 AAIII (80.0%) and 7/10 sGBM (70.0%). *MTSS1* methylation was significantly more frequent in *IDH1* mutated samples (18/19; 94.7%) compared to *IDH1* wild-type samples (12/39; 30.8%) (Fisher's exact test <0.0001; Fig. 1A and Table 1).

### *MTSS1 is Transcriptionally Down-Regulated in Glioma Cells and in a Subgroup of Primary Tumor Tissues*

Real time RT-PCR analysis was used to investigate RNA expression level transcriptional activity of the gene in primary glioma tissues and derived cell lines. Reduced or no expression was found in

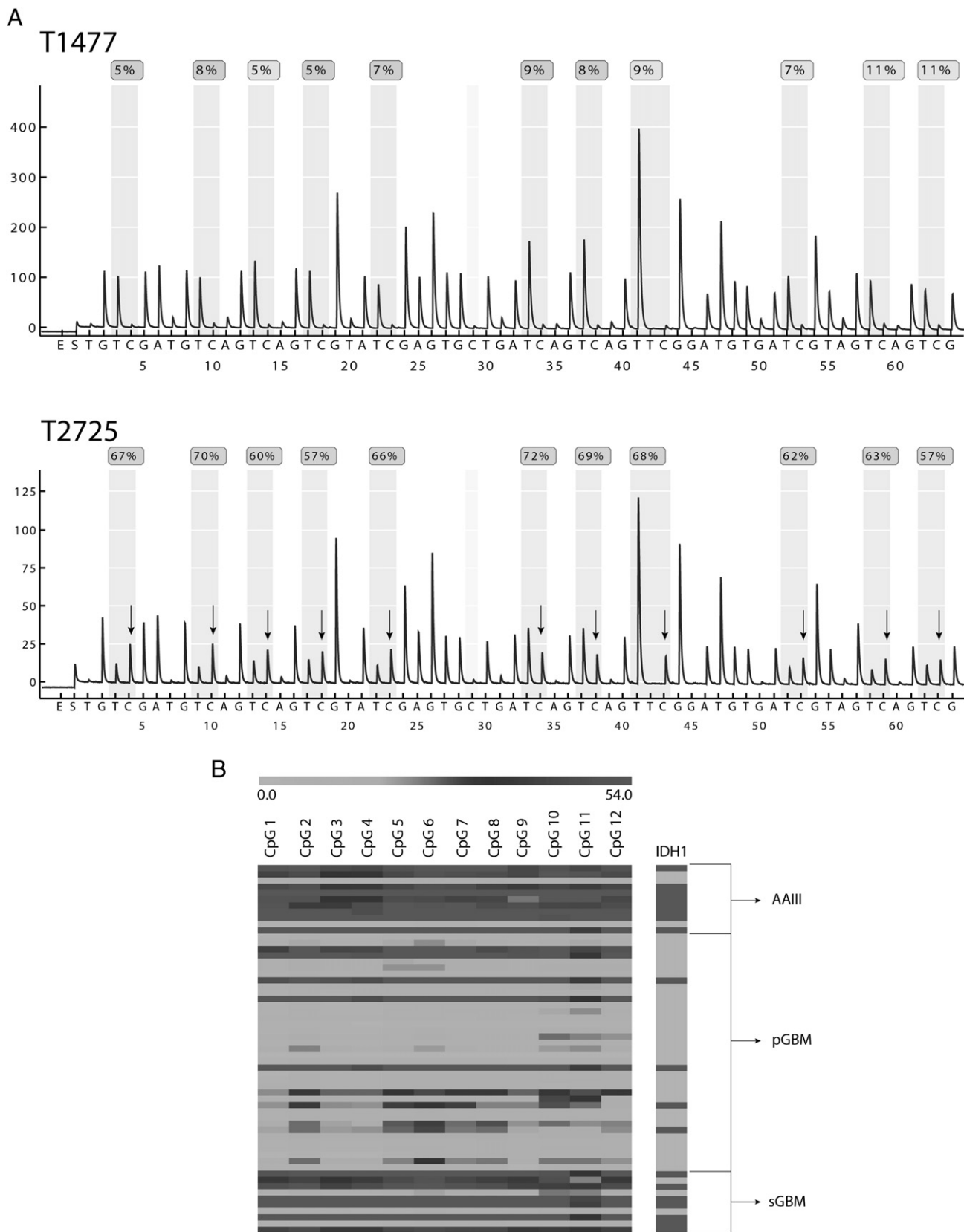


**Fig. 1.** A: Representative pyrosequencing analysis of the *MTSS1* CpG sites. The pyrograms show methylation frequencies for 11 individual CpG sites within the CpG Island associated with the *MTSS1* gene. The tissue sample (upper pyrogram) shows an overall methylation level of 8.1%, and is scored as non-methylated, the lower pyrogram the methylated tissue sample (lower pyrogram) 59.1%. Arrows mark the signals of the respective methylation sites. The mean percentages of methylated alleles are noted above the CpG positions. B: Representation of *MTSS1* methylation data Heatmap of DNA methylation of 59 primary glioma samples. (Red: High methylation; Green: Low methylation) as well as *IDH1 R132* mutation status (Red: mutated; Green: not mutated). The threshold of methylation was set to eight-fold SD of white matter control samples (13.8%). 14/38 (36.8%) of pGBM, 9/11 (81.8%) of AIII and 8/10 (80%) of sGBM were detected as methylated. Data indicates a significant higher methylation frequency in sGBM and AIII than in pGBM.

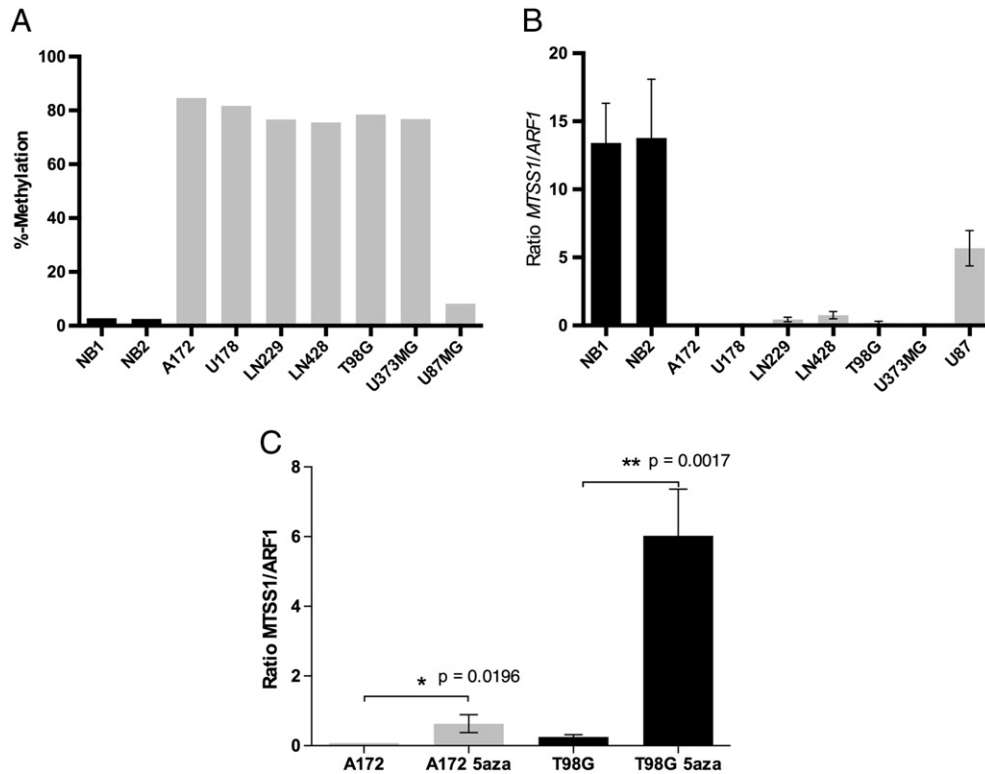


**Fig. 2.** A, B: Methylation and expression of *MTSS1* in glioma cell lines and normal brain tissue. Methylation status of the analyzed glioma cell lines (A). 6/7 lines show high methylation levels of the investigated region in the CpG island upstream of the *MTSS1*-gene. NB: normal brain tissue. Relative *MTSS1*-mRNA expression normalized to *ARF1* (B). U87MG shows endogenous *MTSS1* transcripts in statistically significant difference (as indicated by asterisk) to all other cell lines which do not express *MTSS1*-mRNA and demonstrate a methylated *MTSS1* promoter. C: Demethylation and reactivation of *MTSS1* transcription. Relative transcript levels of *MTSS1* (*MTSS1/ARF1*) in glioblastoma cell lines A172 and T98G without or with 0.5  $\mu$ M 5-aza-2'-deoxycytidine treatment for three days. The demethylating treatment results in significant increase of *MTSS1*-mRNA transcription (A172 8 fold; T98G 24 fold).

cell lines A172, U178, LN229, LN428, T98G, and U373MG. Significant expression of *MTSS1* was exclusively found in U87MG (see Fig. 2B). Treatment of glioma cell lines with 5-aza-2'-deoxycytidine lead to a significant reduction of methylation especially in T98G (51%) and A172 cells (33%) with consecutive increase of mRNA-expression of 24 fold and 8 fold respectively (Fig. 2C). Reduced expression was observed in 18/35 pGBM (51.4%), 0/11 AAI and 1/10 sGBM (10.0%) while normal expression was detected in 10/35 (28.6%) of pGBM, 8/11 (72.7%) AAI and 4/10 sGBM (40%). High levels of *MTSS1* transcripts were detected in 7/35 pGBM (20%), 3/11 AAI (27.3%) and 5/10 sGBM (50%) (Supplementary Fig. 1). There was no significant correlation between methylation status and mRNA expression of *MTSS1* in the investigated primary tumor tissues.

#### Loss of Heterozygosity of *MTSS1* is More Frequent in Secondary Glioblastoma and Anaplastic Astrocytoma as Opposed to pGBM and Correlates with DNA Methylation

To investigate potential losses of the *MTSS1* gene by deletion, we performed comparative SNP-analyses of DNA extracted from tumor tissues and corresponding lymphocytic DNA. LOH was found in 2/9 informative cases of AAI, 2/6 sGBM and 2/20 pGBM. Interestingly, all cases of AAI and sGBM with LOH in the *MTSS1* locus also showed hypermethylation of the gene, while all pGBM tissues with LOH of *MTSS1* are unmethylated at the investigated CpG sites (Table 1). However, due to low number of samples, this correlation does not reach statistical significance (Fisher's exact test:  $P = .0667$ ).

#### *MTSS1* Inhibits Cell Motility and Invasion

To study the impact of *MTSS1* protein expression on the motility and invasion of glioma cell lines, we performed trans-well and scratch assay experiments, respectively. For the scratch assay LN229 cells were stably transfected with *MTSS1*-pEGFP-C1 expression plasmid. LN229-pEGFP-C1 transfected LN229 cells were used as control. Microscopic images taken at different time points (0 h, 12 h and 24 h) show high cell migration capacity of the control cells that filled the empty space in about 24 hours. *MTSS1* overexpressing cells reveal a significant impairment of migration (Fig. 3A).

The transwell-chamber-invasion assay showed comparable results. The percentage of invading LN229 cells was reduced by 36% after transfection with the *MTSS1*-pEGFP-C1 construct (average 7.4 cells/visual field) compared to control cells LN229-pEGFP-C1 cells (11.6 cells/visual field). Fig. 3b shows the relative amount of counted points 2 and 10 hours after seeding.

The results of these two assays provide functional proof for *MTSS1* protein acting as inhibitor of migration/invasion of glioma cells *in vitro*.

#### *MTSS1* is Co-Localized with Actin Filaments

In order to determine protein expression under physiological conditions in normal astrocytes, we generated human astrocytes by *in vitro* differentiation of IPS cells and used immunofluorescence staining for the assessment of subcellular protein localization. Human astrocytes were stained with actin-binding Phalloidin, anti-*MTSS1* antibody and analyzed by fluorescence microscopy. *MTSS1* protein was expressed in filopodia and matrix associated cell-contact

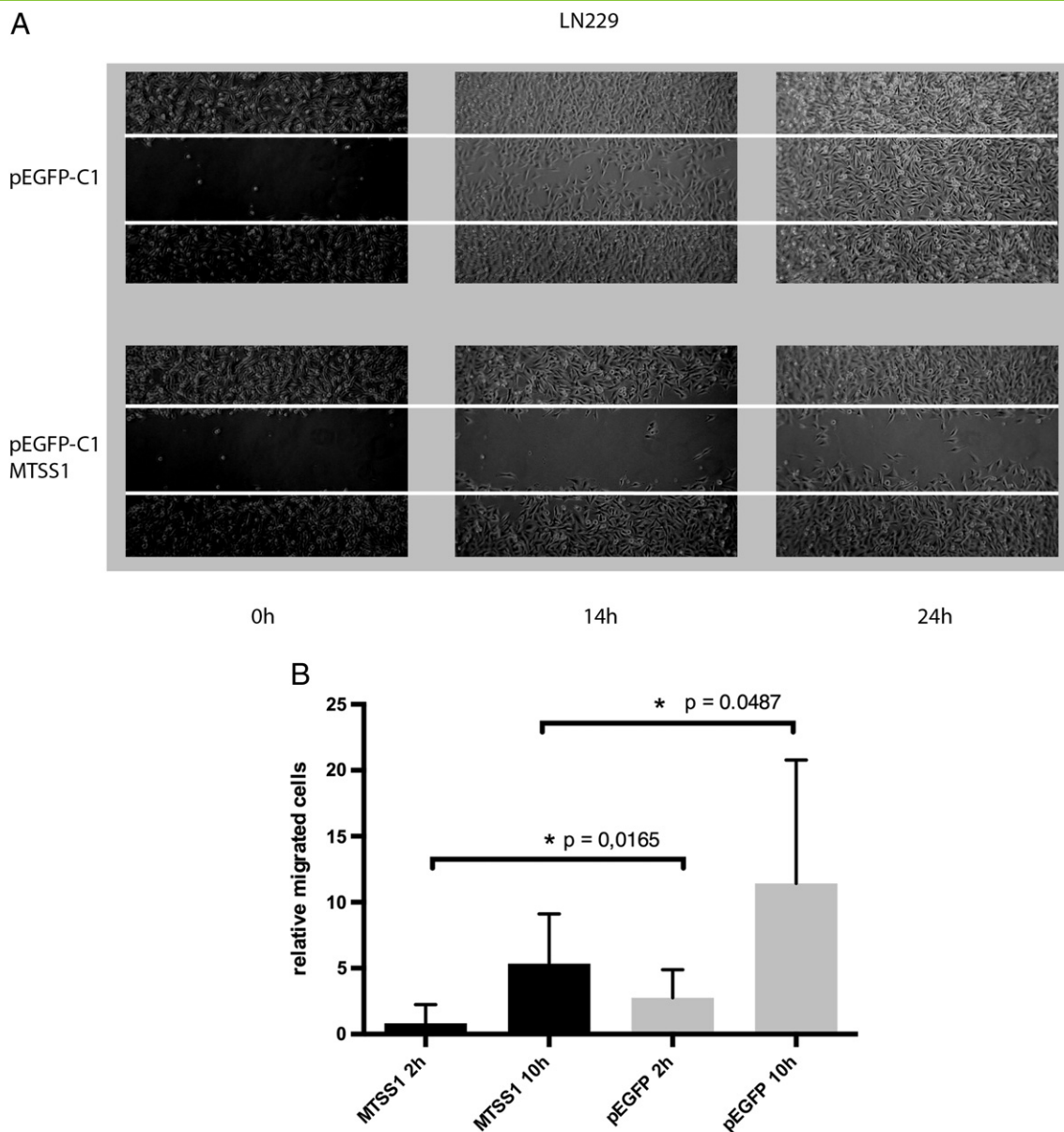


**Fig. 3.** A: Microscopic imaging of the scratch assay. Wounds are indicated by white lines. The upper 3 images show LN229 cells transfected with the empty vector control. LN229 cells transfected with pEGFP-C1 MTSS1 construct are shown in the lower panel. Images were taken immediately after placing the wound, and after 14 and 24 h. B: Transwell-invasion-assay. Relative cell migration through membrane after 2 and 10 hours. LN229-MTSS1-pEGFP-C1 transfected cells show higher relative invasion potential than LN229-pEGFP-C1 control cells. pEGFP-C1 cells were used as 100% mark. LN229-MTSS1-pEGFP-C1 transfected cells only reach 64% after 10 hours of cultivation. Statistical significance is indicated by asterisk and p values.

structures co-localized with actin-filaments (Fig. 5). This localization argues for a functional role of MTSS1 protein in the attachment of astrocytes. Consequently, loss of the protein in glioma cells might influence their motility and invasion capacity.

**MTSS1 Overexpression Does Not Alter Proliferation or Apoptosis**

Cellular proliferation and apoptosis were measured by flow cytometric analysis using antibodies against phospho-(Ser10)-Histone H3 and cleaved-Poly(ADP-ribose)-polymerase (PARP; Asp214) respectively. The proliferation rate of MTSS1 expressing cells was 0.3% and 0.6%, apoptotic rates were 20.8% and 10% in 48 hours. Control cells showed proliferation rates of 0.1% and 0.6% while the fraction of apoptotic cells were 17.7% and 9.7%. No

significant differences in proliferation or apoptotic cells between MTSS1 expressing cells compared to the control cells (Fig. 4) were found, suggesting that the expression of MTSS1 has no significant effect on the apoptosis or proliferation of glioma cells *in vitro*.

**Relationship Between Molecular Findings and Clinical Data**

Forty-seven GBM patients were included in the analysis of MTSS1 methylation and survival. Mean survival of patients with hypermethylation or no methylation of MTSS1 was 780 days and 420 days, respectively. A significant correlation ( $P = .0012$ ) was obtained between hypermethylation of MTSS1 and longer survival of the patients. Forty-five GBM patients were included in the Kaplan–Meier survival analysis and of MTSS1 expression study.

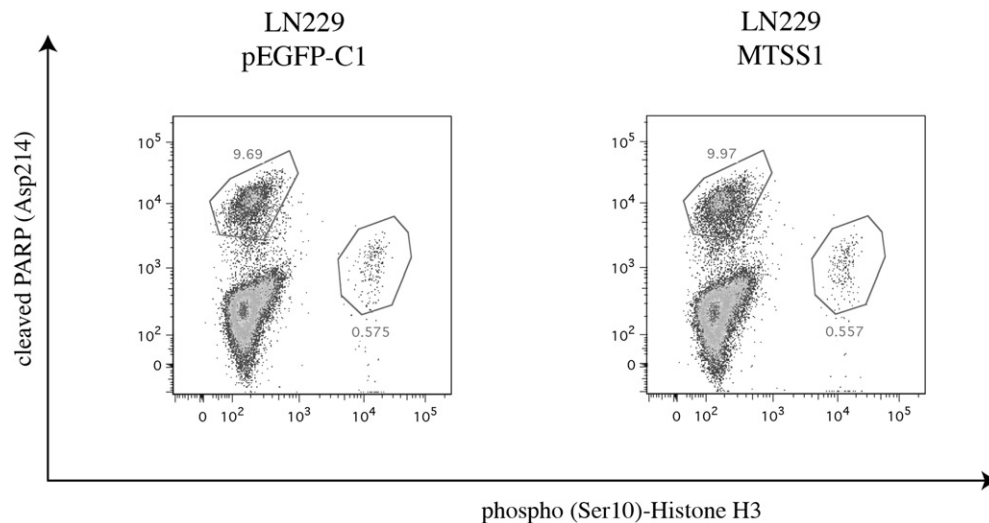


**Fig. 4.** Representative results of flow cytometric analysis. Left: LN229-MTSS1-pEGFP-C1 right: LN229-pEGFP-C1. Overexpression of MTSS1 in LN229 cells does not cause significant differences in cellular proliferation or apoptosis. Proliferation was measured by staining with antibodies against phospho-(Ser10)-histone H3, and apoptosis by staining cleaved PARP(Asp214) respectively.

Mean survival of patients showing expression of MTSS1 was 660 days compared to 330 days for patients showing no or strongly reduced transcription of MTSS1. A significant correlation between MTSS1 transcription and longer survival was seen ( $P = .0113$ ).

## Discussion

Diffuse gliomas are the most common neoplasm of the adult central nervous systems. A hallmark of diffuse gliomas is their capacity to infiltrate surrounding glial tissue. These migratory and invasive properties of glioma cells have a major impact on the poor outcome of glioma patients, prevent a successful treatment of the disease leading to the fact that most patients die within 2 years. Nevertheless, mechanisms implicated in glioma invasion and migration are extremely complex and still not fully understood. In this study, we demonstrated that epigenetic silencing of *MTSS1* may play a role in invasion and migration in diffuse gliomas.

In the seven glioma cell lines used in this study we obtained data suggesting that methylation of the *MTSS1* upstream region suppresses transcriptional activity of the gene. Firstly, methylation status and RNA expression levels of the tumor cell lines indicate a direct negative correlation between methylation and transcript levels, since all but one cell lines revealed a strongly methylated *MTSS1* upstream region with no significant *MTSS1* RNA expression. On the other hand, U87 does not contain a methylated *MTSS1* upstream region and shows mRNA levels comparable to normal brain tissue, which is also unmethylated.

In addition, demethylation of DNA in glioma cells by 5-aza-2'-desoxycytidine treatment, which is frequently used to support epigenetic regulation of gene transcription demonstrated a significant up-regulation of RNA expression in the originally hypermethylated cell lines. These results are in line with previously published data on prostate cancer cell lines [16] and suggest that methylation of the promoter region inactivates *MTSS1* transcription.

*MTSS1* methylation was found in 14/38 (36.8%) pGBM, 9/11 (81.8%) AAI and 8/10 (80%) sGBM. Methylation of *MTSS1* is significantly associated with *IDH1* mutation as investigated by pyrosequencing as well as immunostaining with an R132H specific

antibody indicating that *MTSS1* belongs to those sequences methylated in the G-CIMP phenotype. In line with these findings and with published data on clinical relevance of *IDH1* mutational status, the overall survival of the patients whose tumors show *MTSS1* methylation as well as those containing *IDH1* mutation is significantly longer.

Transcript levels of *MTSS1* comparable to normal tissues were detected in 17/35 (48.6%) of pGBM, 11/11 (100%) of AAI and 9/10 (90%) of sGBM. In contrast to the findings *in vitro*, data obtained from primary tumor tissues does not show a negative impact of methylation on *MTSS1* transcript levels or protein expression. Interestingly, if overall survival is correlated with expression of *MTSS1* mRNA in the tumor tissues, it reveals a positive correlation suggesting that DNA methylation rather promotes *MTSS1* transcription in *IDH1* mutant gliomas with a G-CIMP phenotype. Since a previous study [16] provided evidence, that the 5'-upstream fragment contains promoter activity which is silenced by DNA methylation, it appears, that the cellular context determines if methylation of a particular DNA sequence renders localized genes transcriptionally inactive or not.

Due to conflicting information on *MTSS1* in different tumor types [10–13], the physiological function of the protein and the consequences of its inactivation in tumor cells is not entirely understood. Functional studies indicate that the *MTSS1* protein is able to bind and bundle actin filaments with the WH2-domain and IMD (IRSp53 MIM domain) [7–9]. Saarikangas et al. verified that *MTSS1* is required for actin assembly and integrity [27]. Callahan et al. demonstrated that *MTSS1* acts as a signaling protein in the SHH pathway where it promotes Gli-dependent transcription [14]. Dawson et al. described that *MTSS1* regulates EGFR signaling by enhancing the localization of EGF-receptor to the plasma membrane in low cell density HNSCC tumors but has opposite effects at high cell densities [15].

Here, we analyzed the effects of *MTSS1* overexpression on glioblastoma cell lines. Protein expression in transfected cells leads to a significant reduction of cell motility in scratch assay and trans-well-invasion assay. These data provide further evidence for



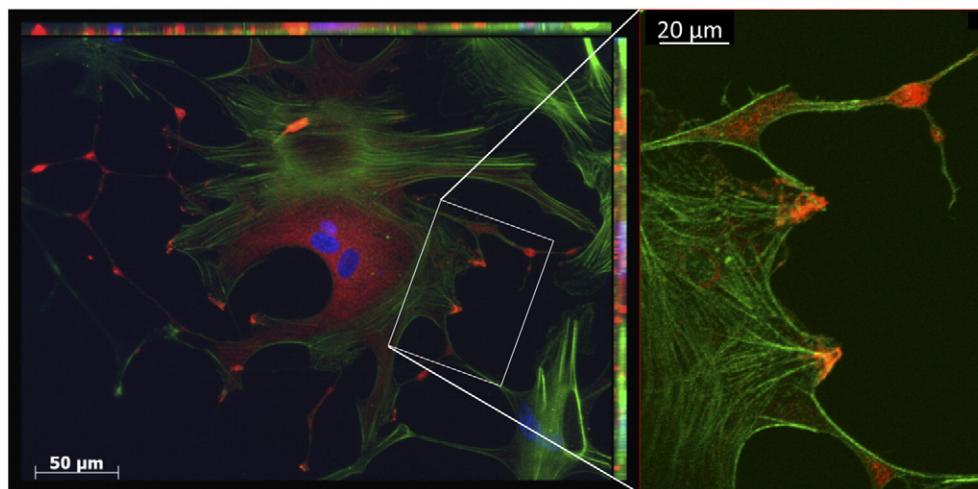


**Fig. 5.** Immunofluorescent detection of MTSS1 in human astrocytes. Top: Human astrocytes induced by IPS cells and stained with actin-binding Phalloidin (green) and MTSS1 (red). Bottom (left): Enlargement; MTSS1 is associated with cell-membrane/focal contact structures as well as actin fibers.

*MTSS1* acting as a tumor suppressor in gliomas and supports its anti-metastatic role. To confirm that the scratch- and trans-well-invasion assay was not influenced by *MTSS1* signaling that alter proliferative or apoptotic behavior of *MTSS1* transfected cells, we also performed FACS analysis to examine proliferation rates and apoptosis in transfected cells. We found no significant

differences between overexpressing *MTSS1* transfected cells and control population.

In order to determine the molecular mechanism by which *MTSS1* enhances cellular attachment and reduces migration, we investigated the subcellular localization of the *MTSS1* protein in human astrocytes. We found the protein localized in cell filopodia of human astrocytes as well as transfected glioblastoma cell lines, where it is co-localized with focal contact associated proteins or filopodia stabilizing actin filaments. This finding argues for a role of the *MTSS1* protein in the formation of cell–cell or cell–matrix contacts in astrocytes and supports previous studies of *MTSS1* as a cell contact stabilizing protein [27,28]. There is, however, evidence that *MTSS1* may also function as a transcriptional regulator in glioma cells *e.g.* of the cortactin *CTTN*-gene [19].

In summary, we report on epigenetic down-regulation of *MTSS1* in glioblastoma cell lines and add the investigated sequence to the G-CIMP phenotype in primary glioma tissues. Our data on normal human astrocytes suggest a function of the protein at focal contact structures with an impact on migratory capacity but no influence on apoptosis or cellular proliferation. Interestingly, in primary glioma tissues, there is no association between *MTSS1* promoter methylation and mRNA or protein expression but a significant impact of mRNA expression on overall survival of glioblastoma patients.

Supplementary data to this article can be found online at <http://dx.doi.org/10.1016/j.tranon.2016.11.006>.

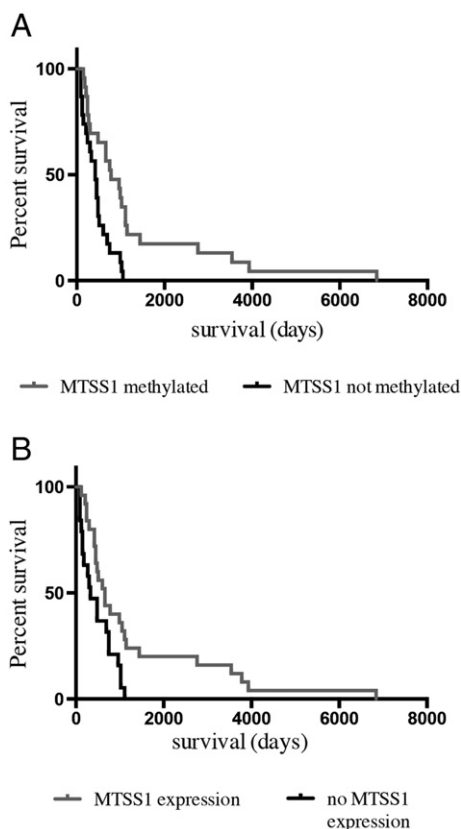


**Fig. 6.** Kaplan–Meier survival analysis. The correlation of *MTSS1* hypermethylation (A) and *MTSS1* transcription (B) with overall survival of GBM patients are statistically significant ( $P = .0012$  and  $P = .0113$  respectively).

## References

- [1] Kleihues P, Louis DN, Scheithauer BW, Rorke LB, Reifenberger G, Burger PC, and Cavenee WK (2002). The WHO Classification of Tumors of the Nervous System. *J Neuropathol Exp Neurol* **61**, 215–225.
- [2] Ohgaki H and Kleihues P (2007). Genetic pathways to primary and secondary glioblastoma. *AJPA* **170**, 1445–1453.
- [3] Parsons DW, Jones S, Zhang X, Lin JC-H, Leary RJ, Angenendt P, Mankoo P, Carter H, Siu IM, and Gallia GL, et al (2008). An Integrated Genomic Analysis of Human Glioblastoma Multiforme. *Science* **321**, 1807–1812.
- [4] Yan H, Parsons DW, Jin G, McLendon R, Rasheed BA, Yuan W, Kos I, Batinic-Haberle I, Jones S, and Riggins GJ, et al (2009). IDH1 and IDH2 Mutations in Gliomas. *N Engl J Med* **360**, 765–773.

- [5] Noushmehr H, Weisenberger DJ, Diefes K, Phillips HS, Pujara K, Berman BP, Pan F, Pelloski CE, Sulman EP, and Bhat KP, et al (2010). Network T. C. G. A. R. Identification of a CpG Island Methylator Phenotype that Defines a Distinct Subgroup of Glioma. *Cancer Cell* **17**, 510–522.
- [6] Waha A, Rodrigues FJ, Waha A, Waha A, Meyer-Puttlitz B, Cavenee WK, Huang TH-M, Wiestler OD, and Yan PS (2004). Methylation Profiling Identifies Epigenetic Markers for High-grade Gliomas. *Cancer Genomics Proteomics* **1**, 209–214.
- [7] Mattila PK, Salminen M, Yamashiro T, Lappalainen P, and Mouse MIM (2003). a tissue-specific regulator of cytoskeletal dynamics, interacts with ATP-actin monomers through its C-terminal WH2 domain. *J Biol Chem* **278**, 8452–8459.
- [8] Woodings JA, Sharp SJ, and Machesky LM (2003). MIM-B, a putative metastasis suppressor protein, binds to actin and to protein tyrosine phosphatase delta. *Biochem J* **371**, 463–471.
- [9] Millard TH, Bompard G, Heung MY, Dafforn TR, Scott DJ, Machesky LM, and Futterer K (2005). Structural basis of filopodia formation induced by the IRSp53/MIM homology domain of human IRSp53. *EMBO J* **24**, 240–250.
- [10] Lee YG, Macoska JA, Korenchuk S, and Pienta KJMIM (2002). a potential metastasis suppressor gene in bladder cancer. *Neoplasia* **4**, 291–294.
- [11] Liu K, Wang G, Ding H, Chen Y, Yu G, and Wang J (2010). Downregulation of metastasis suppressor 1 (MTSS1) is associated with nodal metastasis and poor outcome in Chinese patients with gastric cancer. *BMC Cancer* **10**.
- [12] Wang D, M-R X, Wang T, Li T, and Zhu JW (2011). MTSS1 Overexpression Correlates with Poor Prognosis in Colorectal Cancer. *J Gastrointest Surg* **15**, 1205–1212.
- [13] Parr C and Jiang WG (2009). Metastasis suppressor 1 (MTSS1) demonstrates prognostic value and anti-metastatic properties in breast cancer. *Eur J Cancer* **45**, 1673–1683.
- [14] Callahan CA, Ofstad T, Horng L, Wang JK, Zhen HH, Coulombe PA, and Oro AE (2004). MIM/BEG4, a Sonic hedgehog-responsive gene that potentiates Gli-dependent transcription. *Genes Dev* **18**, 2724–2729.
- [15] Dawson JC, Timpson P, Kalna G, and Machesky LM (2012). Mtss1 regulates epidermal growth factor signaling in head and neck squamous carcinoma cells. *Oncogene* **31**, 1781–1793.
- [16] Utikal J, Gratchev A, Muller-Molinet I, Oerther S, Kzhyshkowska J, Arens N, Grobholz R, Kannoakadan S, and Goerdts S (2006). The expression of metastasis suppressor MIM/MTSS1 is regulated by DNA methylation. *Int J Cancer* **119**, 2287–2293.
- [17] Fan H, Chen L, Zhang F, Quan Y, Su X, Qiu X, Zhao Z, Kong KL, Dong S, and Song Y, et al (2012). MTSS1, a novel target of DNA methyltransferase 3B, functions as a tumor suppressor in hepatocellular carcinoma. *Oncogene* **31**, 2298–2308.
- [18] Schemionek M, Herrmann O, Reher MM, Chatain N, Schubert C, Costa IG, Hänzelmann S, Gusmao EG, Kintsler S, and Braunschweig T, et al (2015). Mtss1 is a critical epigenetically regulated tumor suppressor in CML. *Leukemia* **30**, 823–832.
- [19] Zhang S and Qi Q (2014). MTSS1 suppresses cell migration and invasion by targeting CTTN in glioblastoma. *J Neurooncol* **121**, 425–431.
- [20] Louis DN, Ohgaki H, Wiestler OD, Cavenee WK, Burger PC, Jouvet A, Scheithauer BW, and Kleihues P (2007). The 2007 WHO Classification of Tumours of the Central Nervous System. *Acta Neuropathol* **114**, 97–109.
- [21] Ichimura K, Schmidt EE, Goike HM, and Collins VP (1996). Human glioblastomas with no alterations of the CDKN2A (p16INK4A, MTS1) and CDK4 genes have frequent mutations of the retinoblastoma gene. *Oncogene* **13**, 1065–1072.
- [22] Waha A, Felsberg J, Hartmann W, Knesebeck v, dem A, Mikeska T, Joos S, Wolter M, Koch A, and Yan PS, et al (2010). Epigenetic Downregulation of Mitogen-Activated Protein Kinase Phosphatase MKP-2 Relieves Its Growth Suppressive Activity in Glioma Cells. *Cancer Res* **70**, 1689–1699.
- [23] Hartmann W, Kuchler J, Koch A, Friedrichs N, Waha A, Endl E, Czerwitzi J, Metzger D, Steiner S, and Wurst P, et al (2009). Activation of phosphatidylinositol-3'-kinase/AKT signaling is essential in hepatoblastoma survival. *Clin Cancer Res* **15**, 4538–4545.
- [24] Setty P, Hammes J, Rothämel T, Vladimirova V, Kramm CM, Pietsch T, and Waha AA (2010). Pyrosequencing-Based Assay for the Rapid Detection of IDH1 Mutations in Clinical Samples. *J Mol Diagn* **12**, 750–756.
- [25] Falk A, Koch P, Kesavan J, Takashima Y, Ladewig J, Alexander M, Wiskow O, Tailor J, Trotter M, and Pollard S, et al (2012). Capture of Neuroepithelial-Like Stem Cells from Pluripotent Stem Cells Provides a Versatile System for In Vitro Production of Human Neurons. *PLoS ONE* **7**, e29597–e29613.
- [26] Koch P, Breuer P, Peitz M, Jungverdorben J, Kesavan J, Poppe D, Doerr J, Ladewig J, Mertens J, and Tüting T, et al (2011). Excitation-induced ataxin-3 aggregation in neurons from patients with Machado–Joseph disease. *Nature*, 1–6.
- [27] Saarikangas J, Mattila PK, Varjosalo M, Bovellan M, Hakanen J, Calzada-Wack J, Tost M, Jennen L, Rathkolb B, and Hans W, et al (2011). Missing-in-metastasis MIM/MTSS1 promotes actin assembly at intercellular junctions and is required for integrity of kidney epithelia. *J Cell Sci* **124**, 1245–1255.
- [28] Dawson JC, Bruche S, Spence HJ, Braga VMM, and Machesky LM (2012). Mtss1 Promotes Cell-Cell Junction Assembly and Stability through the Small GTPase Rac1. *PLoS ONE* **7**.